



Original Article

Development and validation of a fast sub-channel code for LWR multi-physics analyses

Khurram Saleem Chaudri ¹, Jaeha Kim, Yonghee Kim*

Department of Nuclear and Quantum Engineering, Korea Advanced Institute of Science and Technology (KAIST), 291 Daehak-ro, Yuseong-gu, 34141, Republic of Korea

ARTICLE INFO

Article history:

Received 3 January 2019

Received in revised form

5 February 2019

Accepted 22 February 2019

Available online 27 February 2019

Keywords:

Sub-channel

LWR

PSBT

Thermal hydraulics

Multi-physics analyses

START

ABSTRACT

A sub-channel solver, named **S**tudy of **R**eactor **T**hermal **H**ydraulics (START), has been developed using the homogenous model for two-phase conditions of light water reactors. The code is developed as a fast and accurate TH-solver for coupled and multi-physics calculations. START has been validated against the NUPEC PWR Sub-channel and Bundle Test (PSBT) database. Tests like single-channel quality and void-fraction for steady state, outlet fluid temperature for steady state, rod-bundle quality and void-fraction for both steady state and transient conditions have been analyzed and compared with experimental values. Results reveal a good accuracy of solution for both steady state and transient scenarios. Axially different values for turbulent mixing coefficient are used based on different grid-spacer types. This provides better results as compared to using a single value of turbulent mixing coefficient. Code-to-code evaluation of PSBT results by the START code compares well with other industrial codes. The START code has been parallelized with the OpenMP algorithm and its numerical performance is evaluated with a large whole PWR core. Scaling study of START shows a good parallel performance.

© 2019 Korean Nuclear Society, Published by Elsevier Korea LLC. This is an open access article under the CC BY-NC-ND license (<http://creativecommons.org/licenses/by-nc-nd/4.0/>).

1. Introduction

The need to perform high fidelity analyses for a nuclear reactor in a reasonable time cannot be emphasized enough. To get a true picture of a multitude of interacting physical phenomena in nuclear reactors is a challenging task. Among many interacting physics, thermal hydraulics impact on reactor physics is a prominent one. Regarding the goal of high fidelity multi-physics analyses with the constraint of affordable computational time, sub-channel analyses can satisfy the requirements.

To get an accurate picture of fluid flow in presence of heat addition from a fuel rod, various approaches based on different number of fluid-phase models have been put forward by researchers for the LWRs (Light Water Reactor). Single fluid (homogenous) for two-phase flow [1–3] and two (liquid and gas) or three fluid (liquid, vapor, and entrained droplets) approach [4,5] for two-phase flow are present in literature. For each considered fluid,

a set of conservation equations for energy, momentum (axial and lateral) and mass are solved. Meanwhile, there are also intermediate approaches that consider separate equations for liquid and vapor mass but combined equations for energy and momentum [1]. Each additional term, in terms of the number of phases to model, adds to information obtained on the cost of computational time. Additional complexity in the form of non-condensable gases in the coolant of LWRs can worsen the situation [6] for computational time. Although the CFD (computational fluid dynamics) approach provides a higher-fidelity solution, it is still too much costly for whole-core multi-physics applications, albeit a lot of progress [7].

With the goal of high accuracy in practical computing time, many researchers have relied on the homogenous mixture approach to solve the two-phase flow problems in LWRs. It is well known that the accuracy of the relatively simple mixture model largely depends on thermal hydraulic correlation used in the analysis. These thermal hydraulic correlations are developed from a plethora of data generated by experiments for different set of geometrical and flow conditions. Information including, but not limited to, Critical Heat Flux (CHF), pressure drop, grid spacer effect, sub-cooled boiling, drift-flux etc. can be obtained accurately from such correlations.

* Corresponding author.

E-mail address: yongheekim@kaist.ac.kr (Y. Kim).

¹ Permanent Address: Department of Nuclear Engineering, Pakistan Institute of Engineering and Applied Science (PIEAS), Nilore 45650, Islamabad, Pakistan.

Various approaches are available to model turbulent mixing phenomena in sub-channel geometries. A popular approach is to use an equal mass exchange model, which depends upon the turbulent mixing coefficient, connecting gap width and average mass flux between connected channels [1–3,8]. In order to determine the turbulent mixing coefficient, thermal mixing tests are usually performed in single-phase conditions. Typically a single value of turbulent mixing coefficient is used in the LWR sub-channel analyses [2]. Some other studies have adopted the region-wise value approach [3]. Other codes have applied different correlations based on equal volume exchange and/or void drift [9].

Various sets of experimental data are available for the assessment and validation of sub-channel computer codes. The OECD/NRC benchmark based on NUPPEC PWR Sub-Channel and Bundle Test (PSBT) [10] is a comprehensive experimental database to validate various aspects of thermal hydraulics solvers. It provides experimental results for various single channels and bundles in a very systematic way for both steady-state and transient conditions.

The aim of this work is to develop a fast and accurate sub-channel solver to perform LWR design analyses in the coupled/multi-physics environment. The new sub-channel thermal hydraulics solver, named Steady and Transient Analyzer for Reactor Thermal hydraulics (START), is reported in this work. The START code is based on homogenous equilibrium theory and is equipped with appropriate correlations to get an accurate assessment of various physical phenomena. In order to correctly model the turbulent mixing, a different approach is adopted in this study, i.e., elevation-dependent turbulent mixing coefficients depending on grid-spacer types. The developed solver is validated against the PSBT experimental database. The OpenMP parallel algorithm is implemented in the START code to speed-up the execution time.

2. Solution methodology of the START code

The Study and Transient Analyzer for Reactor Thermal hydraulics (START) code has been developed at Center for Autonomous SMR Research (CASMRR), KAIST. Main features of the code are that it is written in a modular fashion using modern Fortran. Modularity ensures that only addition/editing of certain portions of the code, without disturbing the rest of the solver, new functionalities can be introduced conveniently. For example, the addition of new correlation or ability to handle fluids other than light water as coolant can be easily implemented and maintained. Another advantage of modularity is that the code can be used both as a standalone program for thermal hydraulics and can be very easily implemented as a subroutine also to perform in-memory coupling with neutron physics solvers to perform coupled neutron physics and thermal hydraulics analyses. To decrease the computation time, some of the rank 2 and 3 arrays of the code were vectorized to 1 dimension in order to boost calculation speed.

The START code considers homogenous two-phase model with Equal Velocity (EV) and Equal Temperature (ET) approximations. Conservation equations for mass, energy, momentum (linear and transverse) in finite difference form are solved using well-developed sub-channel formulation. The Newton-Raphson iterative method solves the pressure drop for axial and lateral momentum equations, as this method provides good stability for a solution [1]. Marching type algorithm, similar to the one used in COBRA-IIIC [11] and MATRA [3], is used to solve the set of equations in the START code. Time-dependent calculations are done based on an implicit scheme. The typical coolant centered sub-channel configuration, as shown in Fig. 1, is used to define basic conservation equations. Neutron physics analyses usually consider fuel rod at the center of the channel that can also be termed as rod centered sub-channel. In order to convert coolant centered sub-channel

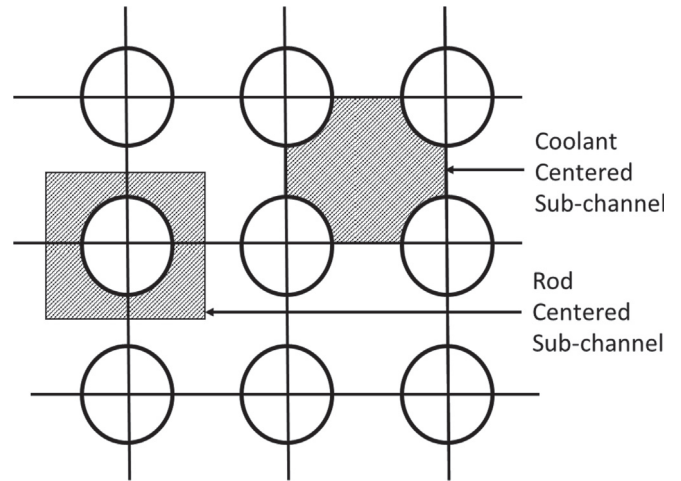


Fig. 1. Sub-channel definition in an array of fuel rods [13].

quantities to rod centered based values, appropriate weighted average over channels neighboring fuel rod under consideration is taken [12].

In equations (1)–(4), subscript i and j stand for lateral sub-channel node indices. Axial direction is considered to be along the z -axis. The transverse flow rate is considered in x -direction which is separated by a gap in the y -direction. Standard donor cell quantities are denoted with $*$ in superscript. SI system based units are considered in the START code.

$$A_i \frac{\partial}{\partial t} \langle \rho_i \rangle + \frac{\Delta m_i}{\Delta z} = - \sum_{j=1}^J W_{ij} \quad (1)$$

where, A is the flow area while $\langle \rho \rangle$ denotes the volume averaged density. Symbol m denotes the mass flow rate while Δz is the height of the axial node. W is the transverse flow rate per unit length between two connected sub-channels which is summed over all J connected sub-channels.

$$\begin{aligned} & A_i \frac{\partial}{\partial t} [\langle \rho h \rangle_i] + \frac{\Delta}{\Delta z} [m_i h_i] \\ &= \langle q'_i \rangle - \sum_{j=1}^J W_{ij}^* [h_i - h_j] - \sum_{j=1}^J W_{ij} \{h^*\} - \sum_{j=1}^J \bar{k}_c \frac{s_{ij}(T_i - T_j)}{l_{ij}} \end{aligned} \quad (2)$$

where, q' is the linear heat generation rate for rods facing channel i , density is denoted by ρ and enthalpy by h . Thermal conductivity for fluid k_c is averaged over the connected sub-channels while the gap width is denoted by s and centroid-to-centroid distance for two connected sub-channels is given as l .

$$\begin{aligned} & \frac{\partial}{\partial t} \langle m_i \rangle + \sum_{j=1}^J W_{ij} \{v^*\} + \frac{\Delta \{m_i v_i\}}{\Delta z} \\ &= -A_i \langle \rho \rangle g_z - A_i \frac{\Delta \{p\}}{\Delta z} - \sum_{j=1}^J W_{ij}^* [v_i - v_j] - \left\{ \frac{F_i}{\Delta z} \right\} \end{aligned} \quad (3)$$

where, axial velocity is denoted as v while g_z is the gravitational acceleration value, and $\Delta \{p\}$ indicates change in the area averaged pressure term. The F_i term is for forces acting on sub-channel i which considers wall friction and pressure drop due to grid spacers.

$$\frac{\partial}{\partial t} \left(W_{ij}^x \right) + \frac{\Delta}{\Delta z} \left(W_{ij}^x \{v\} \right) = -\frac{S_{ij}^y}{l} (\Delta \{p\}_x) - \left\{ \frac{F_{ix}}{l \Delta z} \right\} \quad (4)$$

where, $\Delta \{p\}_x$ denotes the transverse pressure drop between connected channels.

The assumptions used in writing these equations are

- In Equation (2), the energy conservation equation, complete energy deposition is considered in fuel i.e. no portion of fission energy appear directly in sub-channel
- In Equation (2), the energy conservation equation, axial heat conduction in the coolant is neglected
- In Equation (3), the axial momentum equation, pressure work term is not considered

Current limitations of the START code are that it only models square lattices and it cannot model backflow. Also, the boiling curve is modeled up to CHF point in the START code.

The flow diagram for the calculation procedure carried out to solve the conservation equations is shown in Fig. 2. Steady state solution is a special case of a time-dependent solution in which a single time step is considered with a value of $1.0E+18$ s. This approach is similar to COBRA-EN code [1]. For the first time iteration, the input value for heat flux is used. For subsequent time iterations, fuel heat conduction is solved to obtain heat flux value, which will be used in the remainder of calculations for the current time step. After initialization with appropriate conditions for a relevant time step, axial momentum equation is solved iteratively using Newton-Raphson type iterations based on mass conservation criteria. After convergence, lateral momentum balance is carried out with the condition of mass convergence. Once a solution for lateral momentum is obtained, energy balance is carried out to obtain updated enthalpy and temperatures. This procedure is carried for each axial level. After the solution of all the axial levels is obtained, iterative convergence of solution based on temperature values is checked. If convergence is not achieved, the same procedure with now updated information is carried out again. In the case of convergence, next time step calculation is carried out. Same flow of calculations is repeated until the last time step is reached.

The START code can model typical sub-channels present in fuel assemblies like center channel, a center channel with guide thimble, side channel and corner channels. Results based on such different channel type for the sensitivity study for turbulent mixing coefficient are a part of the manuscript. The code also has the ability to model slightly atypical sub-channels like assembly gap and channels neighboring relatively bigger guide thimbles present in APR-1400 fuel assemblies [14]. In the current version of the code, flow through guide thimble and heat transfer between coolant and guide thimble is not considered. At present,

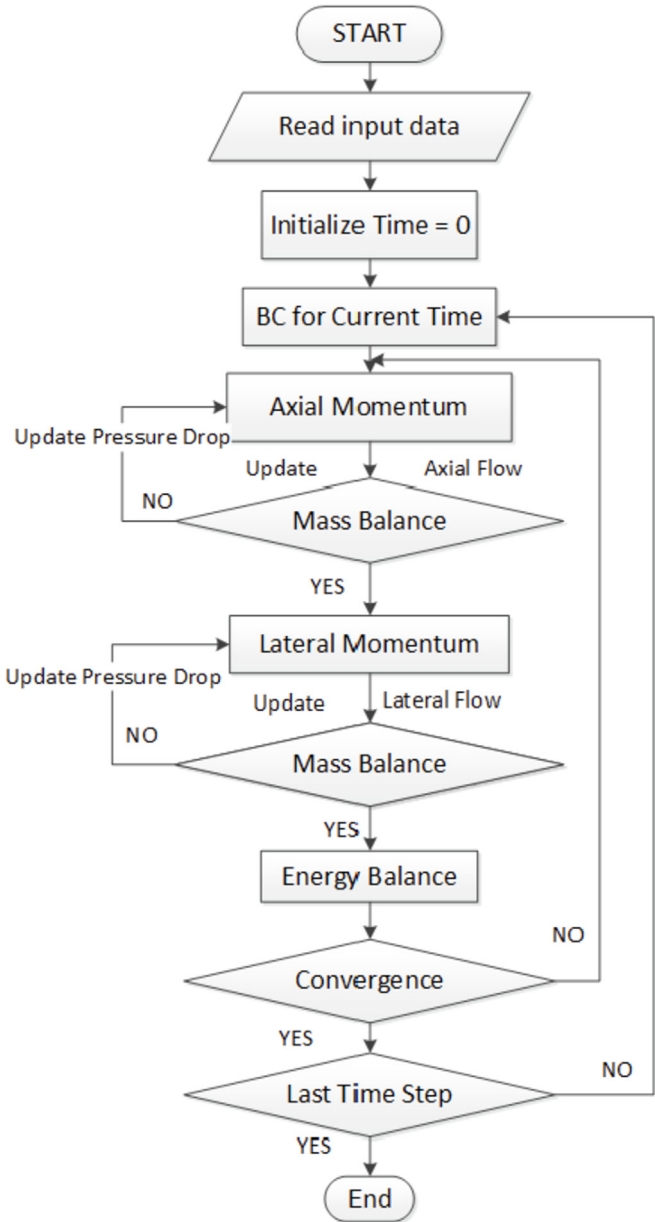


Fig. 2. Calculation flow diagram of the START Code.

guide thimbles are modeled as fuel rods with zero power in the code. In a future version, the capability of flow through guide thimbles and heat transfer between coolant and guide thimble will be added which will help model water rods in BWR and

Table 1
Correlations and models employed in the START code.

Parameter	Correlation
Effective property for homogenous two-phase flow	Awad, M.M. and Muzychka, Y. S [16].
Two-phase friction multiplier	Armand Correlation [1]
Grid spacer pressure drop	K. Rehme Model [17]
Sub-cooled boiling	Lellouche [1]
Void Fraction	Homogenous, Smith, Armand-Massena, Zuber-Findlay [1]
Single phase forced convection HTC	Dittus-Boelter [1]
Subcooled and saturated nucleate boiling HTC	DITTUS + Thom [1]
Turbulent mixing	β determined through thermal mixing test
CHF	EPRI [1]

Table 2

Single sub-channel specification for PSBT.

Item	Data	S1	S2	S3	S4
Sub-channel					
Axial heated length (mm)	1555	1555	1555	1555	
Flow area (mm ²)	107.098	107.098	68.464	42.592	
Heated perimeter (mm)	29.845	22.384	14.923	7.461	
Wetted perimeter (mm)	54.645	54.645	44.923	33.161	
Axial power shape	Uniform	Uniform	Uniform	Uniform	

Table 3

Comparison of different void-fraction correlations.

Model/Correlation	Standard Deviation (SD)	Mean	Root Mean Square (RMS)
Homogenous	6.62E-02	1.47E-02	6.57E-02
Smith	7.59E-02	-7.69E-02	1.06E-01
Armand-Massena	5.92E-02	-3.12E-02	6.52E-02
Zuber-Findlay	4.69E-02	-4.47E-02	6.53E-02

SCWR and also heat transfer between coolant and moderator in CANDU reactors.

Physical and transport properties of light water to be used in the solution of conservation equations are obtained from the International Association for the Properties of Water and Steam (IAPWS-97) Industrial Formulation (2012 Revision-7) [15]. All 5 regions, as defined by IAPWS-97, are available in the code. Considering the modularity of the START code, it can easily be extended to simulate the Super-Critical Water Reactor (SCWR) environment with the addition of suitable correlations. Table 1 lists the main correlations used to model various phenomena in the START code.

3. Benchmarking START against PSBT

3.1. Steady state single channel results

PSBT has provided data to perform the validation of the solvers in a very systematic way i.e. in increasing difficulty/complexity of cases. The first set of data provided is for single sub-channel of different shapes. This gives the opportunity to benchmark the capability of the solution obtained without cross-flow term and grid spacers. Four different kinds of sub-channels i.e. normal central channel (S1), a central channel with instrumentation rod (S2), side channel (S3) and corner channel (S4) are considered. Table 2 provides the specifications of single sub-channel geometry.

To select a suitable correlation for void-fraction determination, four different correlations were compared to select the best performing one. S1 sub-channel studies were repeated using homogenous model, Smith correlation, Armand-Massena correlation, and Zuber-Findlay correlation. Void-fraction statistics for the four mentioned models/correlations are compared in Table 3.

Although the homogenous model shows the smallest value for mean error in Table 3, it is based on the unacceptable assumption that velocity for both liquid and vapors is identical. Hence, we can ignore this minimum mean error obtained with the homogeneous model. The Zuber-Findlay correlation provides a minimum standard deviation among the four approaches. Meanwhile, based on a two-out-of-three parameters criterion, the Armand-Massena correlation results turns out to be best in terms of the mean and RMS

errors. The Armand-Massena correlation used in this work is given in Eq. (5):

$$\alpha = xv_g \frac{(0.833 + 0.167x)}{(1 - x)v_f + xv_g}, \quad (5)$$

where, v_g and v_f are specific volume for gas and liquid phase, respectively. Flow quality is represented by x and void-fraction is given as α .

Also, the positive mean value for homogenous model shows that the homogenous model over-predicts the void-fraction whereas Smith, Armand-Massena, and Zuber-Findlay under-predicts the void-fraction as compared to experimental results. Rest of the results presented in this work are obtained using Armand-Massena correlation. For various geometrical configurations of a single channel, results for quality and void-fraction are compared with PSBT experimental results in Fig. 3. Mean and Standard Deviation (SD) values for single channel calculations are compared with other industry codes, developed by various organizations, in Fig. 4 and Fig. 5.

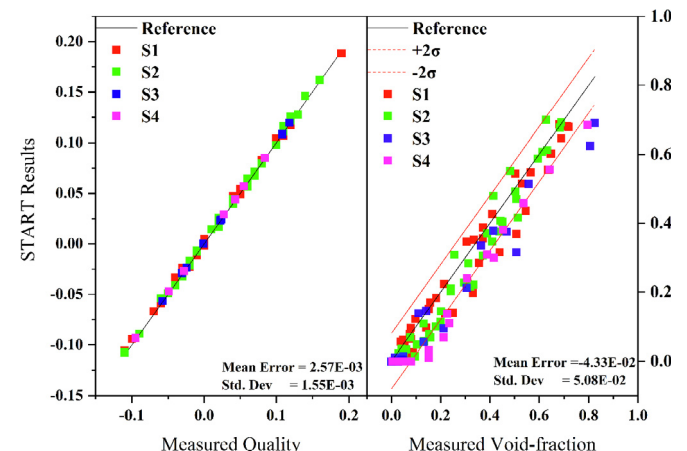


Fig. 3. Single channel quality and void-fraction comparison between START and PSBT data.

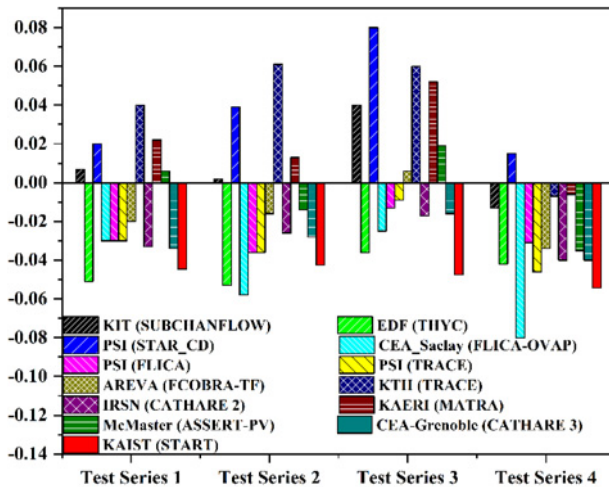


Fig. 4. Mean error of calculated and experimental values difference compared with other codes.

3.2. Determination of turbulent mixing coefficient

In order to tune the turbulent mixing model by selecting an appropriate value of turbulent mixing coefficient, also known as Thermal Diffusion Coefficient (TDC), sub-channel exit fluid temperature test data is provided in the PSBT database under steady-state and single-phase conditions. A 5×5 bundle with a much skewed radial power profile is used for the test, and 17 grid spacers (7 Mixing Vane (MV), 2 Non-Mixing Vane (NMV), and 8 Simple Spacers (SS)) are used over an active height of 3.658 m. Meanwhile, a uniform axial power profile is used in the bundle test. Geometrical data for the bundle is provided in Table 4 and the radial power profile used is shown in Fig. 6. One can note that 12 left-hand side rods are at 100% power, while the others are at 25% relative power.

Different approaches have been used by the researchers to model the turbulent mixing. Some studies have used a single value of turbulent mixing coefficient axially [2]. An optimum value of 0.06, based on exit-coolant temperature predictions staying in ± 10 K envelope of the experimental values, was used in the SUBCHANFLOW code. Other works applied the rather high value of 0.08 for turbulent mixing coefficient [3]. Modification in the form of

Table 4
Geometrical data for bundle A1 used in sub-channel exit temperature test by PSBT.

Item	Data
Rods array	5×5
Number of heated rods	25
Number of thimble rods	0
Heated rod outer diameter (mm)	9.50
Thimble rod outer diameter (mm)	—
Axial heated length (mm)	3658
Axial power shape	Uniform
No. of MV, NMV, and SS	7, 2, 8
Radial power profile	C

using the region-wise β values were applied by the researchers to get a better agreement with experimental data. Using other models for turbulent mixing, researchers have applied various factors depending on the type of grid-spacer and sub-channel. To model this challenging problem, some studies have proposed using CFD-informed models [18]. For large geometries (whole-core scale) with tens of different sub-channels, such approaches can be computationally costly and tedious to implement.

In the current study, the turbulent mixing coefficient value is based on the type of grid spacer and so it can have different values axially. No spacer, SS and NMV were given the same value while MV spacer was allocated a different, higher, β value. A sensitivity study was performed using the same axial value and various different combinations of values for MV and other spacers. The current approach was motivated by the results of CFD studies [18] that show a significantly large lateral convection effect by MV spacers as compared to SS and NMV spacers.

Various sets of values were studied for MV-SS&NMV with the aim of reducing the standard deviation of the exit temperature over 9 data sets to about 5 °C. A value pair of (0.045 & 0.08) was chosen after studies. To see the difference between using one single value of β and grid spacer-dependent value of β , another case was studied with value equal to 0.055, which is the average of all the axial value for the case of 0.045–0.080 case. Although the single value of $\beta = 0.055$ gives a slightly smaller value for mean as compared to the chosen pair of values, the other three parameters i.e. SD, RMS, and percentage of points lying outside ± 10 K envelope values deteriorate. The remaining results presented in this paper are obtained by using 0.045–0.080 value pair of turbulent mixing coefficient. Table 5 lists the results obtained. Fig. 7 plots the exit temperature results for 9 chosen problems by PSBT. It can be noted that data fits well within ± 10 °C range.

Sensitivity study of β also suggests that the results obtained depend on conditions such as pressure, inlet temperature and mass flux. Overall, the mean relative error, for different sub-channel types, is less than 5% for all the 9 problems with maximum error

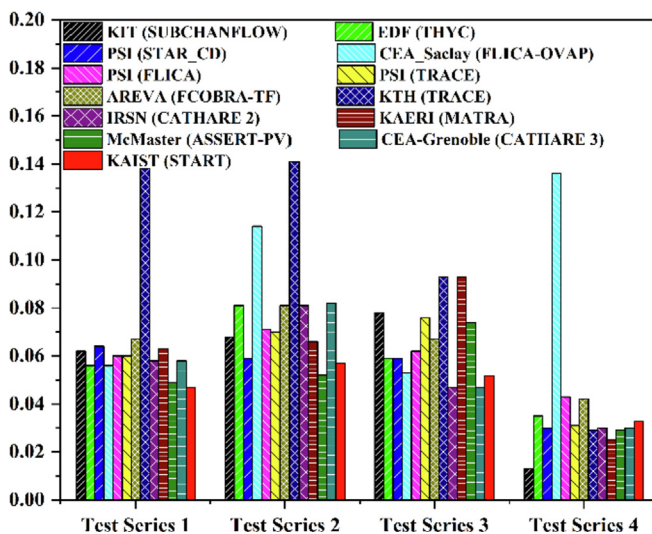


Fig. 5. Code-to-code comparison for standard deviation in results for void-fraction prediction.

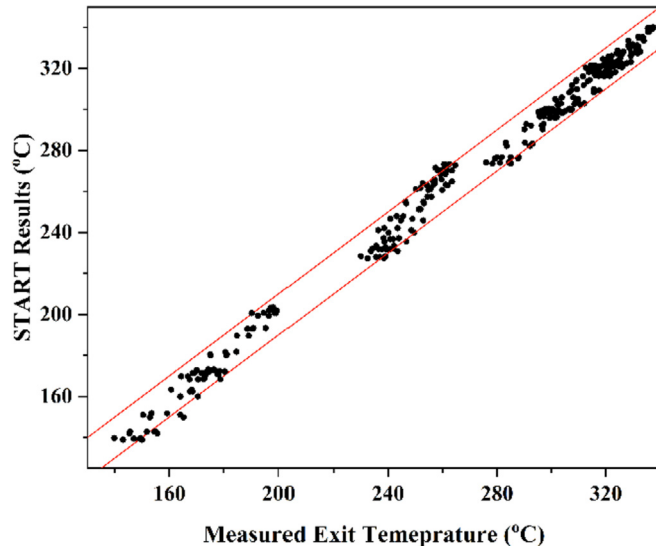
1.00	1.00	0.25	0.25	0.25
1.00	1.00	1.00	0.25	0.25
1.00	1.00	0.25	0.25	0.25
1.00	1.00	1.00	0.25	0.25
1.00	1.00	0.25	0.25	0.25

Fig. 6. Radial power profile-C.

Table 5

Turbulent mixing coefficient sensitivity study statistics.

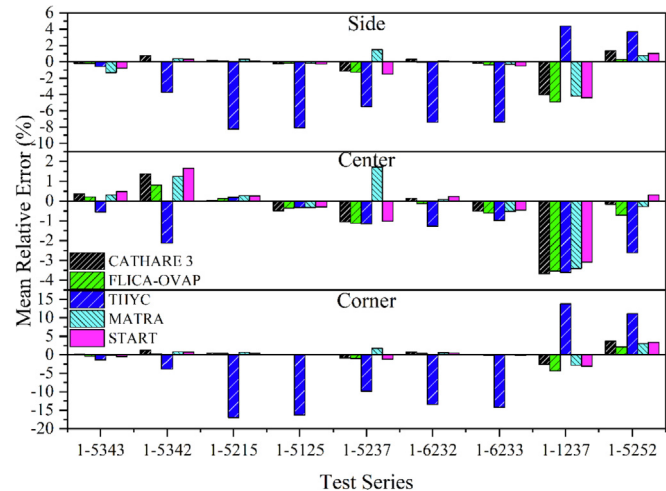
β value	SD (°C)	Mean (°C)	RMS (°C)	% of points with difference > ± 10 °C
0.045–0.080	5.47	−0.69	5.51	8.64
0.055	5.73	−0.65	5.76	9.26

**Fig. 7.** Sub-channel exit temperature comparison for simulated and experimental values.

shown for Test 01–1237 (−4.392% for side channels). Test 01–1237 is conducted at a lower pressure (4.92 MPa) and a lower inlet temperature (86 °C) as compared to other tests. Comparison of mean relative error with other codes for side, center and corner sub-channels is shown in Fig. 8. The comparison shows that START results are quite comparable to those of other codes for all three type of sub-channels, and attesting to the suitability of the chosen value pair of the turbulent mixing coefficient.

3.3. Steady state bundle void distribution

After the selection of appropriate value of the turbulent mixing coefficient, the steady-state void-fraction test for rod-bundles was simulated using the START code and compared with PSBT results of

**Fig. 8.** Code-to-code comparison for outlet temperature by sub-channel type.

thermal quality and void-fraction. Data for 4 different test series labeled 5, 6, 7, and 8 is present in this regard. Geometrical details of these test series are presented in Table 6. Fig. 9 shows radial power distribution A and B used in different test series.

Void-fraction was measured at 3 axial levels i.e. 2216 mm, 2669 mm and 3177 mm from the start of the heated section during the PSBT experiment. These 3 measurements will be labeled as lower, middle and upper-elevation in rest of the manuscript. Average void-fraction value for four sub-channels around the central rod is given by experiment. Fig. 10, Fig. 11, Fig. 12 and Fig. 13 compare the results obtained by the START code with PSBT experimental data. As deduced from earlier results, the Armand-Massena correlation was used for void-fraction determination.

A negative value of mean error shows under-prediction of void-fraction value by the START code as compared to PSBT data. This under-prediction is clear for upper-elevation void-fraction. Similar

Table 6

Geometrical details for rod-bundle void-fraction tests.

Item	Data			
Sub-channel				
	B5	B6	B7	B5
Test series	5, 5T	6, 6T	7, 7T	8
Rods array	5 × 5	5 × 5	5 × 5	5 × 5
Number of heated rods	25	25	24	25
Number of thimble rods	0	0	1	0
Heated rod outer diameter (mm)	9.50	9.50	9.50	9.50
Thimble rod outer diameter (mm)	—	—	12.24	—
Heated rods pitch (mm)	12.60	12.60	12.60	12.60
Axial heated length (mm)	3658	3658	3658	3658
Radial power shape	A	A	B	A
Axial power shape	Uniform	Cosine	Cosine	Uniform
Number of MV/NMV and SS	7,2,8	7,2,8	7,2,8	7,2,8

Type A				
0.85	0.85	0.85	0.85	0.85
0.85	1.00	1.00	1.00	0.85
0.85	1.00	1.00	1.00	0.85
0.85	1.00	1.00	1.00	0.85
0.85	0.85	0.85	0.85	0.85

Type B				
0.85	0.85	0.85	0.85	0.85
0.85	1.00	1.00	1.00	0.85
0.85	1.00	0.00	1.00	0.85
0.85	1.00	1.00	1.00	0.85
0.85	0.85	0.85	0.85	0.85

Fig. 9. Radial power profiles for rod-bundle void-fraction tests.

under-estimations have also been reported by other studies. The negative mean error in the void-fraction is quite common for most of the sub-channel codes, as shown in Fig. 14. It is noteworthy that mean (Fig. 14) and SD (Fig. 15) of the START errors are comparable to those of other codes.

3.4. Transient bundle void distribution

The same geometry as Test series 5, 6 and 7 was used to carry out transient bundle void distribution test, labeled 5T, 6T, and 7T.

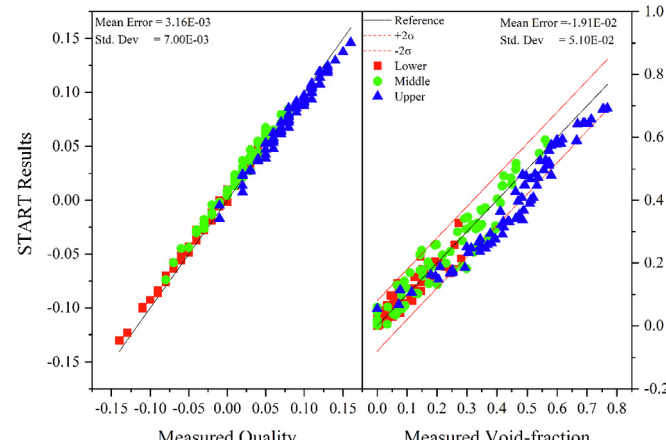


Fig. 10. Test series 5 comparison of START calculated quality and void-fraction with PSBT data.

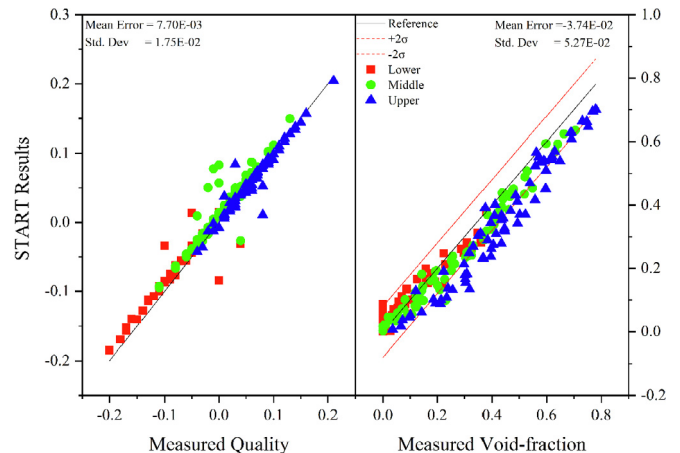


Fig. 11. Test series 6 comparison of START calculated quality and void-fraction with PSBT data.

Geometrical details of these sets are given in Table 6. Lower, middle and upper-elevation measurements for void-fraction value averaged over 4 central sub-channels is provided by the experiment. 4 different scenarios studied for each rod-bundle arrangement are as follows:

1. Power increase
2. Flow reduction
3. Depressurization
4. Inlet temperature increase

Each scenario for three rod bundles i.e. 5T, 6T, and 7T is discussed together.

3.4.1. Power increase transient

Power increase transient scenario for three rod-bundles is presented here. The condition change and the void-fraction trend with respect to time are shown in Fig. 16, Fig. 17 and Fig. 18.

Similar to steady-state test results, lower and middle-elevation values are well compared with experimental data while upper-elevation void-fraction is under-estimated by START. Again, this trend is consistent with results reported by various studies. Time variation trend in void-fraction is followed well by the START code.

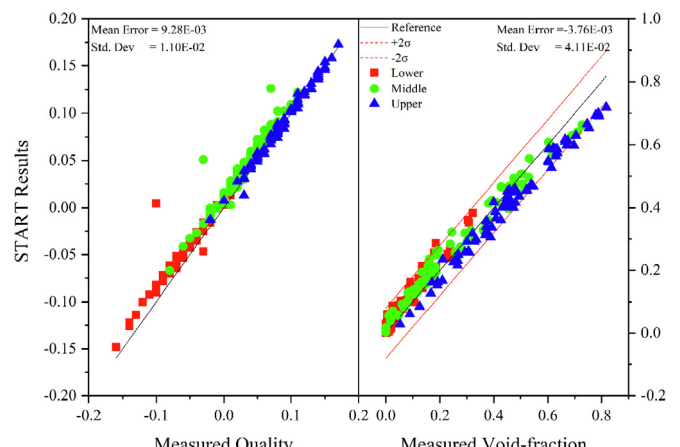


Fig. 12. Test series 7 comparison of START calculated quality and void-fraction with PSBT data.

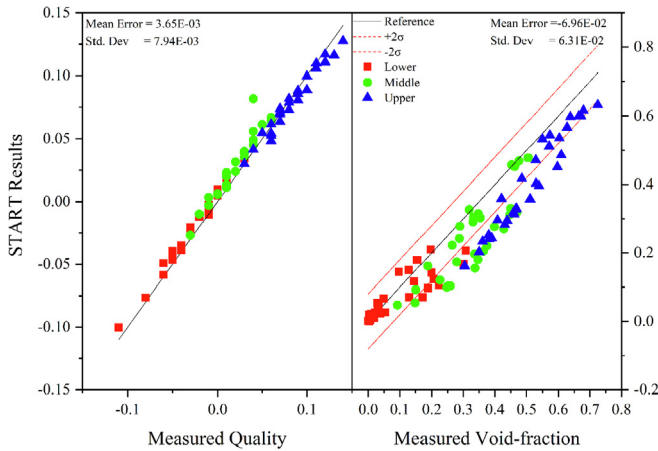


Fig. 13. Test series 8 comparison of START calculated quality and void-fraction with PSBT data.

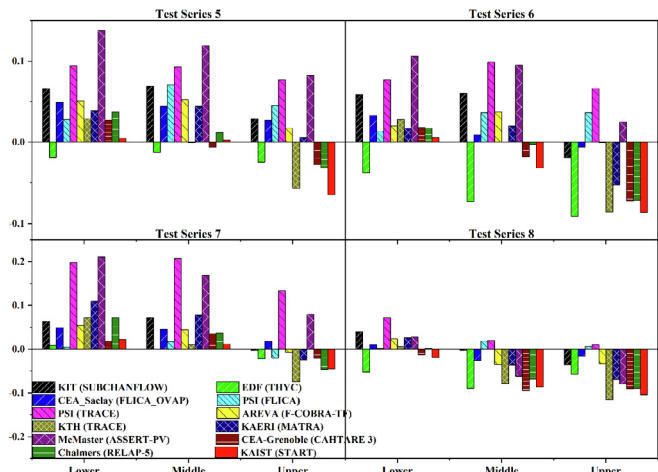


Fig. 14. Code-to-code comparison for bundle test void-fraction mean error.

3.4.2. Flow reduction transient

Keeping inlet pressure, power and inlet temperature to be constant, inlet mass flux for the rod-bundle is reduced to mimic flow reduction phenomenon. Graphs for condition and comparison

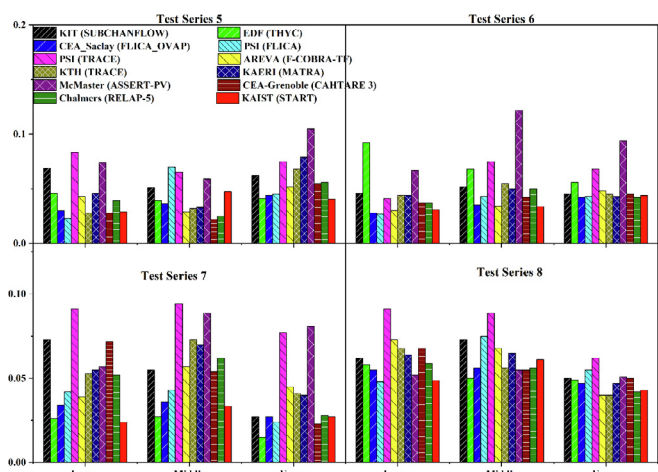


Fig. 15. Standard deviation comparison on code-to-code basis for void-fraction determination.

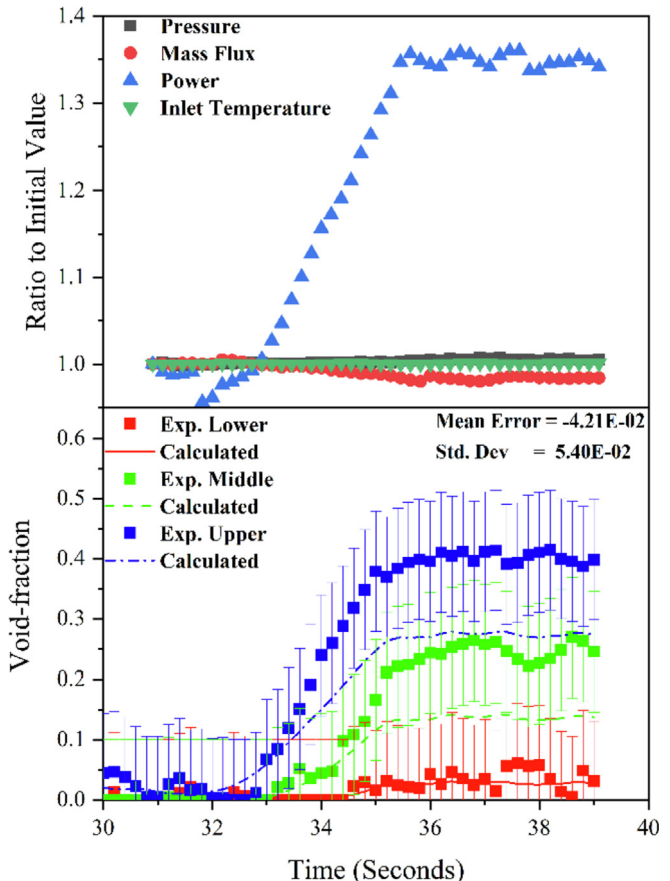


Fig. 16. Power increase transient conditions and void-fraction distribution for test 5T

of void-fraction with PSBT experimental values are presented in Fig. 19, Fig. 20 and Fig. 21 for rod-bundle 5T, 6T, and 7T respectively. The void-fraction trend is similar to that observed for the power increase transient case.

3.4.3. Depressurization transient

Effect of system depressurization on void-fraction was investigated by the PSBT benchmark. Results of START simulation in comparison with experimental values are shown in Fig. 22, Fig. 23 and Fig. 24 along with experimental conditions.

3.4.4. Inlet temperature increase transient

Various studies has deemed experimental conditions for inlet temperature increase transient to be imperfect. Some studies have proposed that thermal capacitance effect of the downcomer region in the experimental setup and location of fluid temperature measurement caused a time delay in the obtained profile [5]. Hence void-fraction for inlet temperature increase transient needs to be shifted forward in time. Different studies have used different time-shifting of 6 or 10-second [19,20]. In this study, time data for START-calculated void-fraction is advanced by 6 s in all three cases. Comparison of un-advanced results and advanced results for 5T case is shown in Fig. 25. Comparison of the 6-second shifted results for 5T, 6T and 7T are presented in Fig. 26, Fig. 27 and Fig. 28 along with experimental conditions.

Collectively, looking at the 4 transient scenarios of three rod-bundles tests (5T, 6T, and 7T), it can be mentioned that 7T results agree closely with experimental values while the other two, 5T and 6T, show larger deviations. Time trend is followed well by the

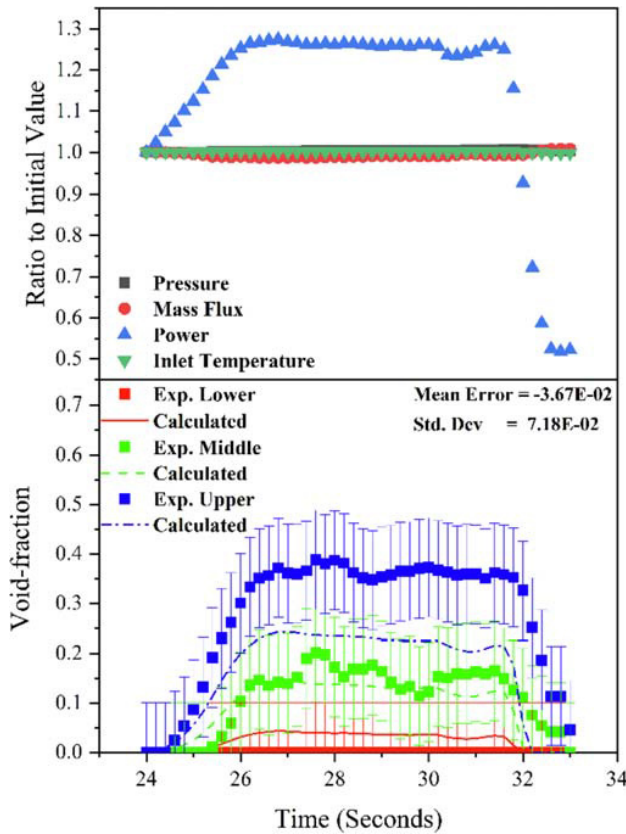


Fig. 17. Power increase transient conditions and void-fraction distribution for test 6T

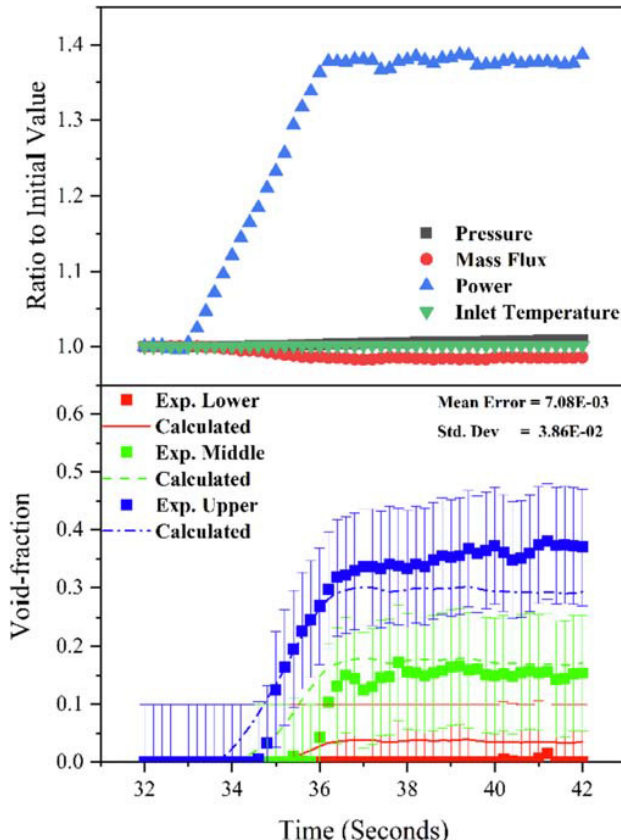


Fig. 18. Power increase transient conditions and void-fraction distribution for test 7T

START code, except inlet temperature increase transient due to faulty experimental conditions. Meanwhile, slight shifting of obtained data to align it with experimental values also gives satisfactory results in the inlet temperature increase case. One can also note that in the power increase case, void-fraction at middle and upper elevation is under-estimated for all three bundles, i.e., 5T, 6T and 7T. In the case of the flow reduction transient, deviation in 5T and 6T is larger while 7T agrees quite well with experimental data. The depressurization case shows larger deviation from experimental value for all three bundles. Results for the inlet temperature increase case shows good agreement for 7T case. Slightly larger deviation in cases 5T and 6T are seen. Code-to-code comparison reveals similar trends reported by other studies yet no reason for the differences is found [19]. This suggests that START performs as well as other sub-channel codes and general agreement with experimental results is satisfactory.

4. OpenMP parallelization of the START code

In order to achieve the goal of multi-physics analyses of full-scale PWR in a practical time, OpenMP parallelization has been applied to various parts of the START code. A large PWR core with 241 fuel assemblies is considered to check the performance of the implemented OpenMP algorithm in the START code. The fuel assembly is a typical 17×17 design and the whole-core sub-channel analysis was done with a few geometrical simplifications, which include no coolant flow through guide tubes, no inter-assembly gap, and a small wall clearance for channels at core boundary.

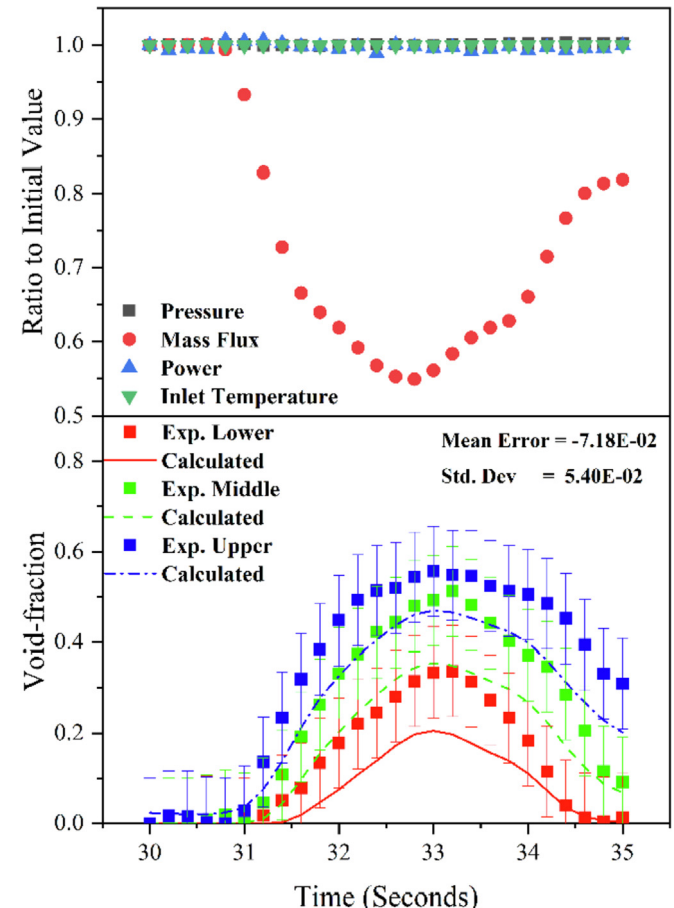


Fig. 19. Flow reduction transient conditions and void-fraction distribution for test 5T

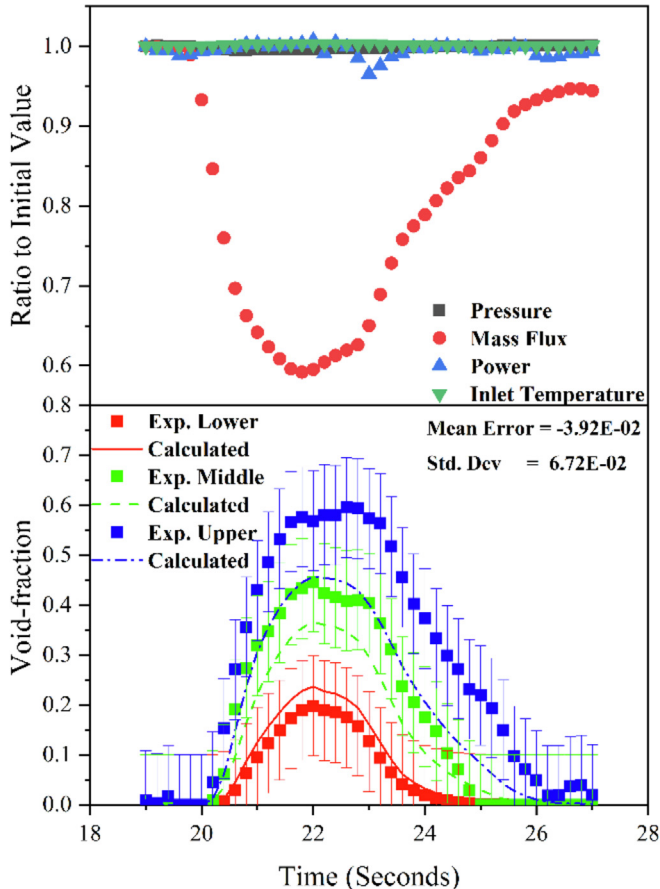


Fig. 20. Flow reduction transient conditions and void-fraction distribution for test 6T

Also, no grid spacers are considered in this analysis as detailed power distribution was determined by an in-house neutronics code [21] without any grid spacers. The START analysis here is one-way, i.e., a pre-determined power profile is used in the sub-channel analysis. The whole PWR core contains a total of 70,228 sub-channels.

The current analysis is performed with typical PWR parameters for flow rate ($3500 \text{ kg/m}^2\text{-sec}$), inlet temperature (290.6°C) and pressure (15.5 MPa). In each sub-channel, 18 axial nodes are considered for the active height of 3.658 m. Fig. 29 shows the axially-integrated power profile in the whole core, which was used to perform the thermal hydraulics analyses. It is mentioned that many control rods were actually partially inserted in the core and the radial and axial power peaking is 2.13 and 1.51, respectively, in the power distribution.

The large whole-core sub-channel analysis was performed on a small parallel computer with Intel Xeon Gold 6148 CPU of 2.40 GHz, which has 40 computational cores for parallel computing. Although a large number of sub-channels are considered in the analysis, the START code worked well without any numerical problems. The results for coolant exit density are shown in Fig. 30. In accordance with the power profile, the assemblies with high power production are showing lower coolant density in sub-channels. It is noted that sub-channel density decrease is quite limited in the core boundary region due to very low power density in the region.

Computing time for the whole core analysis is 42.65 min on a single core of the parallel computer. After implementation of the OpenMP algorithm, the same calculation was repeated using 10, 20,

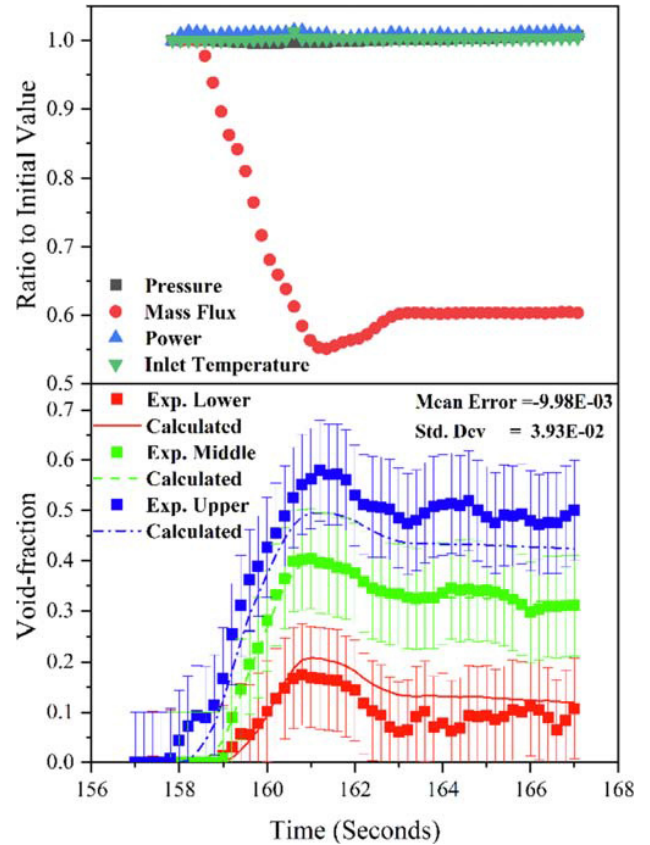


Fig. 21. Flow reduction transient conditions and void-fraction distribution for test 7T

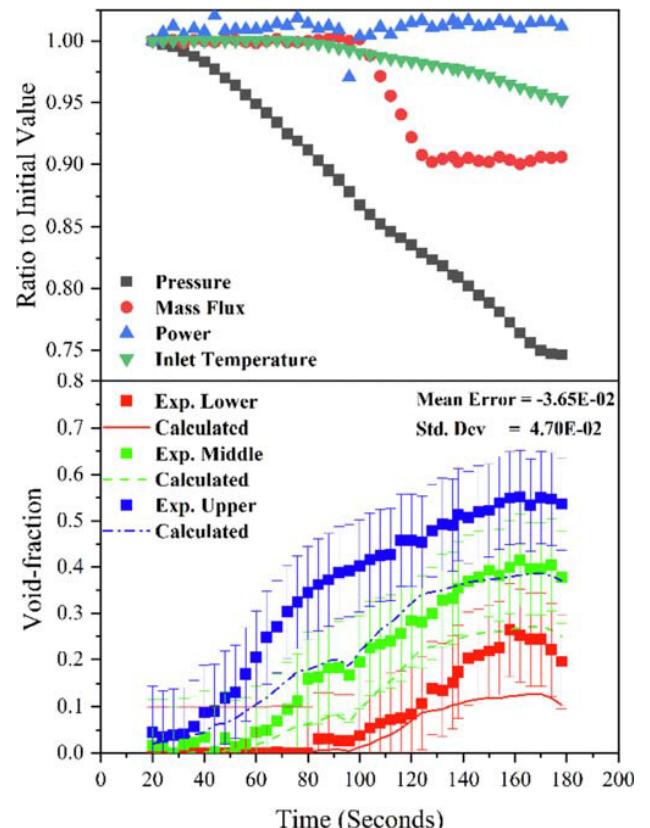


Fig. 22. Depressurization transient conditions and void-fraction distribution for test 5T

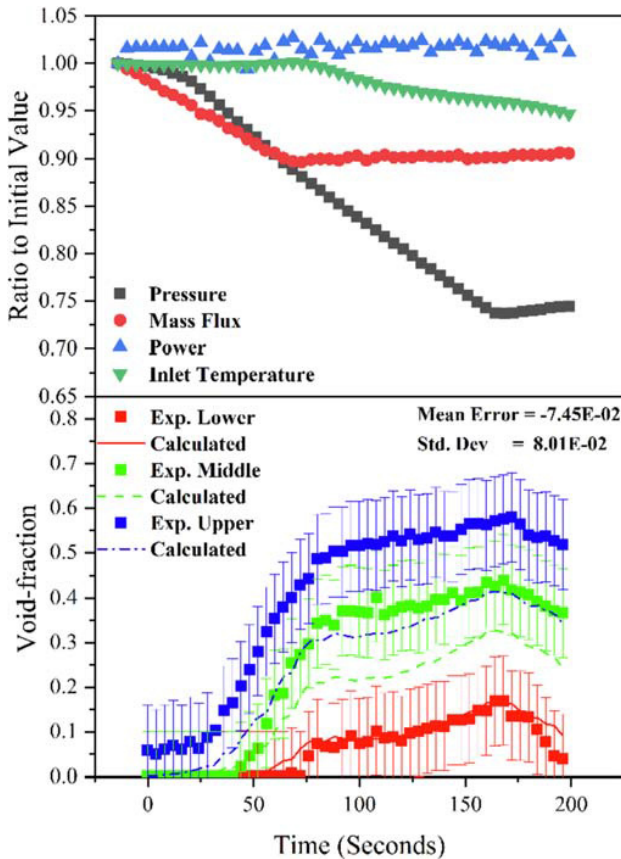


Fig. 23. Depressurization transient conditions and void-fraction distribution for test 6T

30 and 40 cores, and the speed-up results are shown in Fig. 31. One can note that the parallel speed-up is almost linear up to 10 cores and a speed-up of 31.2, corresponding to 78% parallel efficiency, is obtained with 40 cores, i.e., START takes 1.37 min to solve the problem with 40 cores. Fig. 31 indicates that the START code works quite well with the simple OpenMP algorithm.

In multi-physics LWR analyses, a number of iterations for thermal hydraulics and other interacting physics are performed. The core conditions for these iterations are not very different once the solution is close to convergence. Consequently, parts of the converged solution in the previous iteration can be used as the initial conditions in the current iteration, and the sub-channel computing cost can be reduced a lot. Pressure distribution and flow rates from the previous iteration were used as initial conditions for the current iteration in this study. To see impact of the initial guess on the computing time, after convergence of the whole core sub-channel analysis, the reactor power was increased uniformly by 1% and the sub-channel analysis was done again. It was found that a speedup of about 1.9 could be achieved with the better initial guess and the second analysis required only about 44 s.

5. Conclusions

Based on the homogenous equilibrium two-phase sub-channel model, a thermal hydraulics code named START has been developed. START has been validated using the PSBT single-channel and rod-bundle data for both steady-state and transient calculations. It has been confirmed that results of the START code agree well with experimental results for both steady and transient cases. The effect of turbulent mixing due to grid-spacers can be quite better

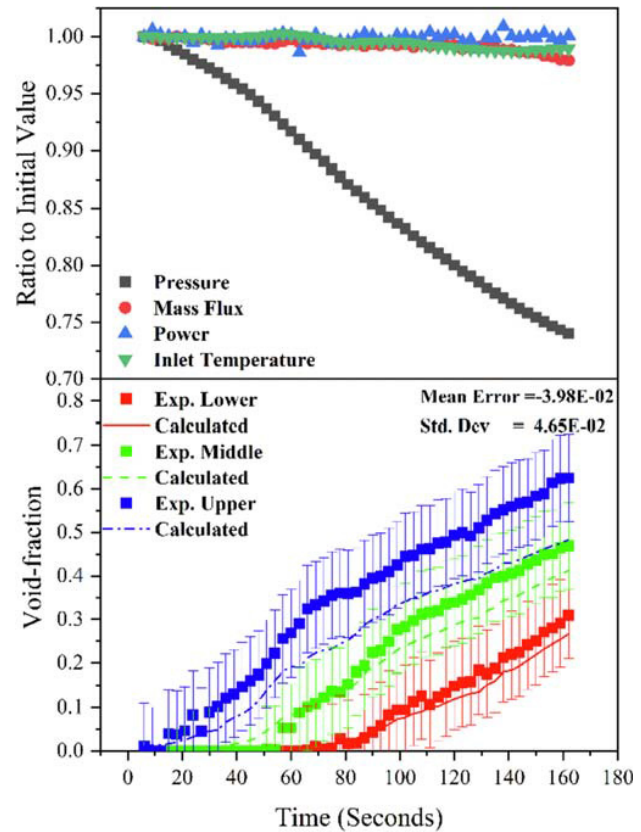


Fig. 24. Depressurization transient conditions and void-fraction distribution for test 7T

modeled by using axially varying values of turbulent mixing coefficients instead of a single value. We also found that START compares well with other industrial codes in terms of the major thermal hydraulic parameters. The START algorithm can be well parallelized with the simple OpenMP algorithm, resulting in about 80% parallel efficiency with 40 cores. Validation and performance of the START code give us the confidence that it can be used as a tool for the multi-physics LWR analysis.

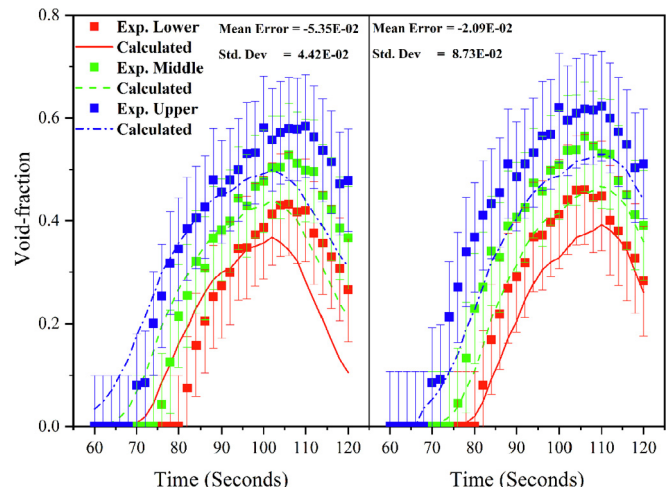


Fig. 25. Un-shifted and 6-second shifted results comparison with experimental values.

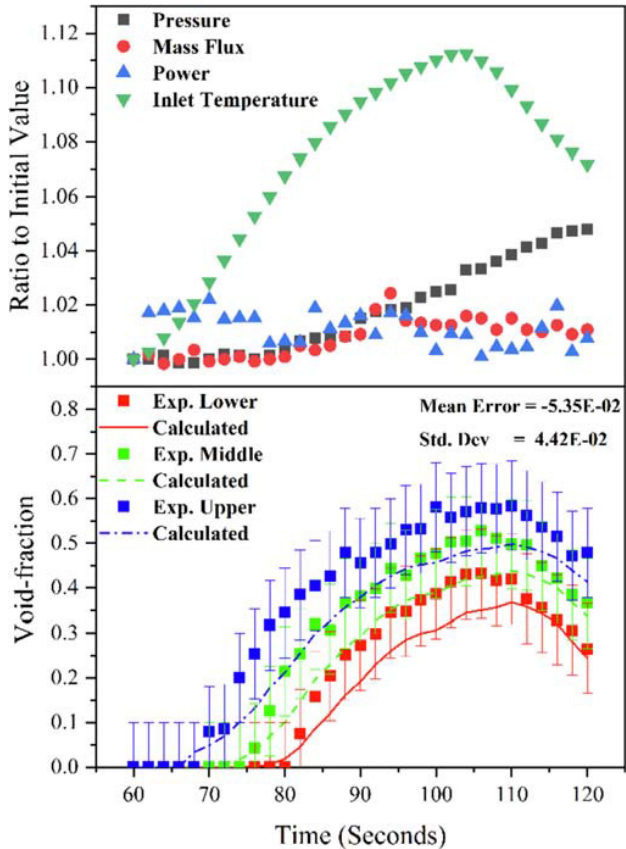


Fig. 26. Inlet temperature increase transient conditions and void-fraction distribution for test 5T

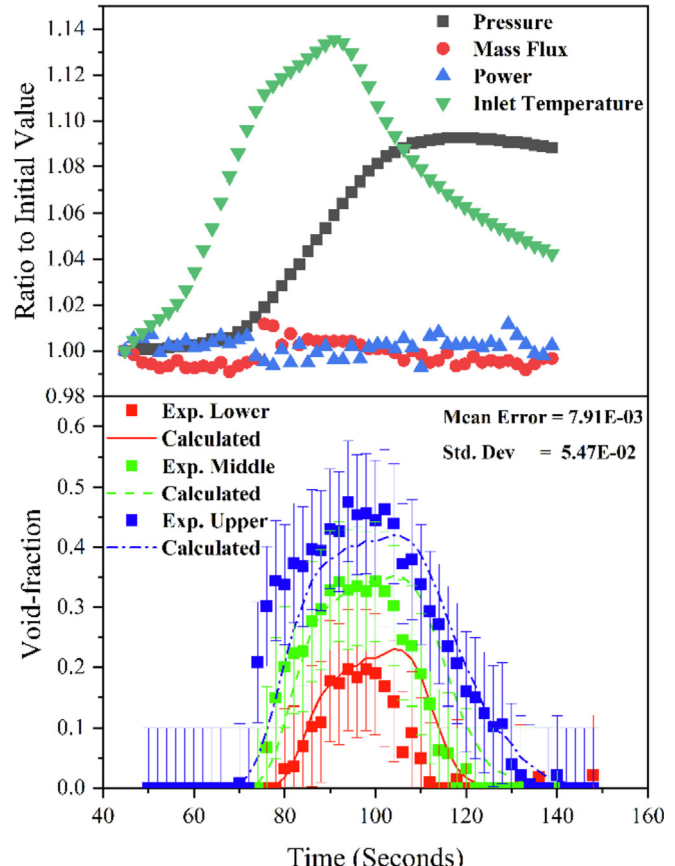


Fig. 28. Inlet temperature increase transient conditions and void-fraction distribution for test 7T

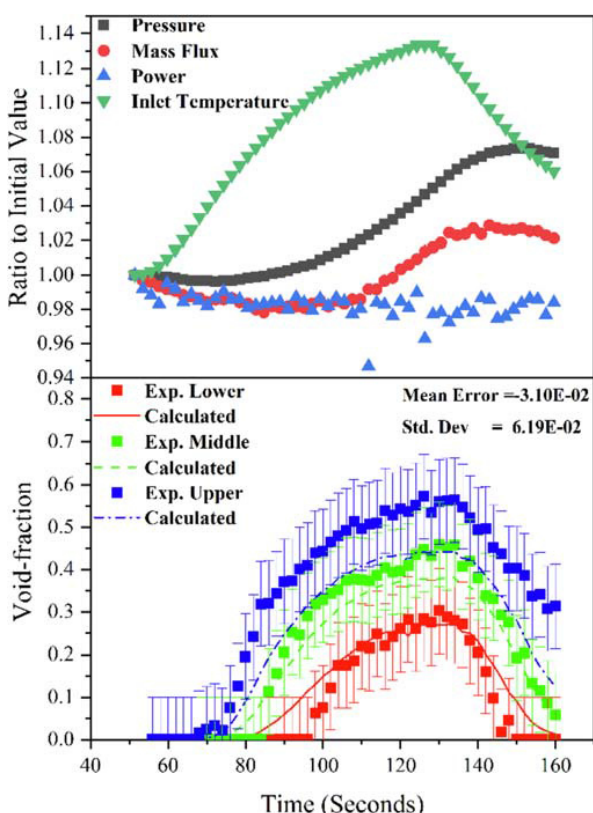


Fig. 27. Inlet temperature increase transient conditions and void-fraction distribution for test 6T

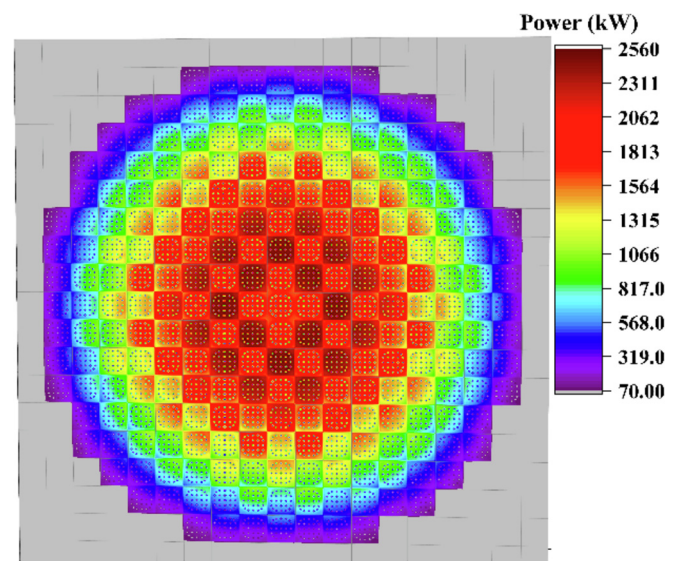


Fig. 29. Radial power profile in a whole core pin-by-pin TH calculation.

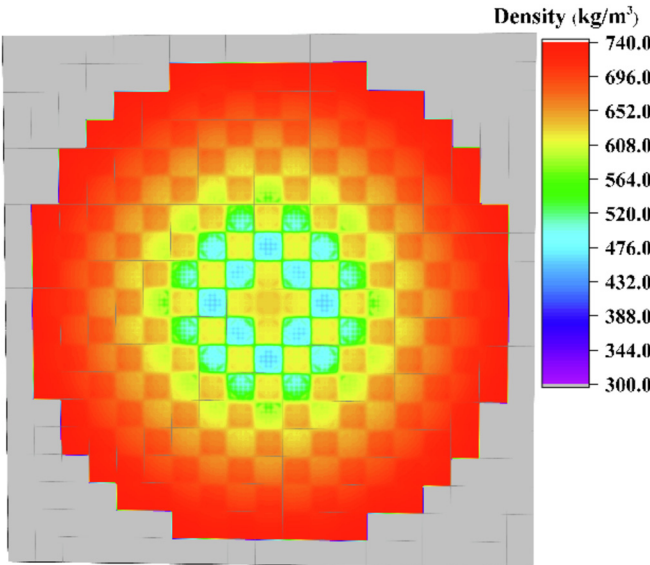


Fig. 30. Coolant sub-channel density results at core exit for pin-by-pin calculation.

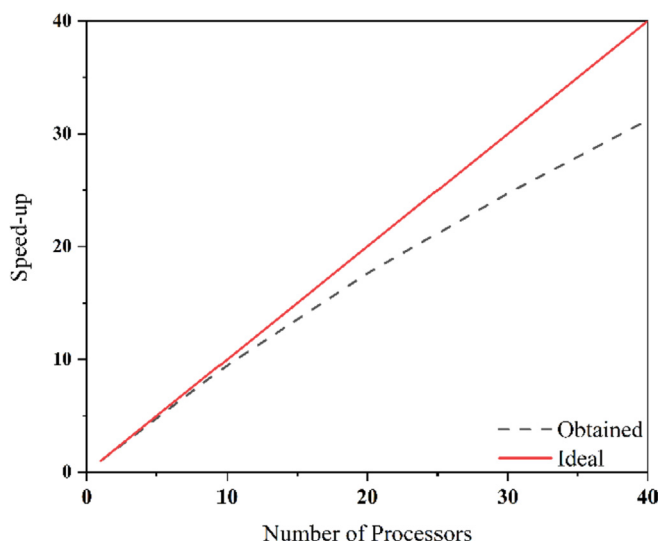


Fig. 31. Parallel performance of START with OpenMP implementation.

Acknowledgment

This work was supported by the National Research Foundation (NRF) of Korea Grant funded by the Korean government (MSIP) (NRF-2016R1A5A1013919).

References

- [1] D. Basile, M. Beghi, R. Chierici, E. Salina, E. Brega, COBRA-EN: an upgraded version of the COBRA-3C/MIT code for thermal hydraulic transient analysis of light water reactor fuel assemblies and cores, Radiat. Saf. Inf. Comput. Center, Oak Ridge Natl. Lab. (1999).
- [2] U. Imke, V.H. Sanchez, Validation of the subchannel code SUBCHANFLOW using the NUREG PWR tests (PSBT), Sci. Technol. Nucl. Install. 2012 (2012), <https://doi.org/10.1155/2012/465059>.
- [3] D.-H. Hwang, S.-J. Kim, K.-W. Seo, H. Kwon, Accuracy and uncertainty analysis of PSBT benchmark exercises using a subchannel code MATRA, Sci. Technol. Nucl. Install. (2012) 1–13, <https://doi.org/10.1155/2012/603752>, 2012.
- [4] J.E. Kelly, S.P. Kao, M.S. Kazimi, THERMIT-2 : a Two-Fluid Model for Light Water Reactor Subchannel Transient Analysis, Massachusetts Institute of Technology, Energy Laboratory, Cambridge, Mass, 1981, p. 1981. <http://hdl.handle.net/1721.1/60460>.
- [5] M. Avramova, A. Velazquez-Lozada, A. Rubin, Comparative analysis of CTF and TRACE Thermal-Hydraulic codes using OECD/NRC PSBT benchmark void distribution database, Sci. Technol. Nucl. Install. 2013 (2013), <https://doi.org/10.1155/2013/725687>.
- [6] P. Kral, J. Hyvärinen, A. Prošek, A. Guba, Sources and effect of non-condensable gases in reactor coolant system of LWR, in: 16th Int. Top. Meet. Nucl. React. Therm. NURETH-16, Chicago, 2015, pp. 5194–5208.
- [7] F. Roelofs, V.R. Gopala, L. Chandra, M. Viellieber, A. Class, Simulating fuel assemblies with low resolution CFD approaches, Nucl. Eng. Des. 250 (2012) 548–559. <https://doi.org/10.1016/j.nucengdes.2012.05.029>.
- [8] Y. Sung, R.L. Oelrich, C.C. Lee, N. Ruiz-Esquide, M. Gambetta, C.M. Mazufri, Benchmark of subchannel code VIPRE-W with PSBT void and temperature test data, Sci. Technol. Nucl. Install. (2012), 2012. Article ID 757498, 11 pages. <https://doi.org/10.1155/2012/757498>.
- [9] K.H. Leung, D.R. Novog, Evaluation of ASSERT-PV V3R1 against the PSBT benchmark, Sci. Technol. Nucl. Install. (2012), 2012. Article ID 863503, 21 pages. <https://doi.org/10.1155/2012/863503>.
- [10] M. Avramova, A. Rubin, H. Utsuno, Overview and discussion of the OECD/NRC benchmark based on NUREG PWR subchannel and bundle tests, Sci. Technol. Nucl. Install. (2013) 1–20, <https://doi.org/10.1155/2013/946173>, 2013.
- [11] J.W. Jackson, N.E. Todreas, COBRA IIIC/MIT-2: a Digital Computer Program for Steady State and Transient Thermal-Hydraulic Analysis of Rod Bundle Nuclear Fuel Elements. Final Report, Massachusetts Inst. Of Tech, Energy Lab., Cambridge (USA), 1981.
- [12] A. Bennett, N. Martin, M. Avramova, K. Ivanov, Impact of Radial Void Fraction Distribution on Boiling Water Reactor Lattice Physics Calculations: Application to AREVA's Next Generation BWR Fuel As-Sembly, the ATRIUM™ 11 Design, 2016.
- [13] N.E. Todreas, M.S. Kazimi, Nuclear Systems II: Elements of Thermal Hydraulic Design, Taylor & Francis, 1990.
- [14] S.J. Yoon, S.B. Kim, G.C. Park, H.Y. Yoon, H.K. Cho, Application of CUPID for subchannel-scale thermal-hydraulic analysis of pressurized water reactor core under single-phase conditions, Nucl. Eng. Technol. 50 (2018) 54–67. <https://doi.org/10.1016/j.net.2017.09.008>.
- [15] W. Wagner, H.-J. Kretzschmar, International Steam Tables—Properties of Water and Steam Based on the Industrial Formulation IAPWS-IF97: Tables, Algorithms, Diagrams, and CD-ROM Electronic Steam Tables—All of the Equations of IAPWS-IF97 Including a Complete Set of Supplementary Backward, Springer Science & Business Media, 2007.
- [16] M.M. Awad, Y.S. Muzychka, Effective property models for homogeneous two-phase flows, Exp. Therm. Fluid Sci. 33 (2008) 106–113, <https://doi.org/10.1016/j.expthermflusci.2008.07.006>.
- [17] K. Rehme, Pressure drop of spacer grids in smooth and roughened rod bundles, Nucl. Technol. 33 (1977) 314–317, <https://doi.org/10.13182/NT77-A31793>.
- [18] T.S. Blyth, Development and Implementation of CFD-Informed Models for the Advanced Subchannel Code CTF, 2017.
- [19] A. Rubin, M. Avramova, OECD/NRC Benchmark Based on NUREG PWR Subchannel and Bundle Tests (PSBT). Volume II: Benchmark Results for the Void Distribution Phase, NEA/NSC/DOC, 2011.
- [20] M. Bucci, P. Fillion, Analysis of the NUREG PSBT tests with FLICA-OVAP, Sci. Technol. Nucl. Install. 2012 (2012), <https://doi.org/10.1155/2012/436142>.
- [21] J. Kim, Y. Kim, Development of 3-D HCMFD algorithm for efficient pin-by-pin reactor analysis, Ann. Nucl. Energy 127 (2019) 87–98. <https://doi.org/10.1016/j.anucene.2018.11.035>.